

## Optimal Design of Cylindrical Electrode Using Neural Network Modeling for Electrochemical Finishing

Nadhim M. Faleh

Mechanical Engineering Department, College of Engineering, Al-mustansiriyah University

### Abstract

The finishing operation of the electrochemical finishing technology (ECF) for tube of steel was investigated. In this study, experimental procedures included qualitative and quantitative analyses for surface roughness and material removal. Qualitative analyses utilized finishing optimization of a specific specimen in various design and operating conditions; value of gap from 0.2 to 10mm, flow rate of electrolytes from 5 to 15 liter/min, finishing time from 1 to 4 min and the applied voltage from 6 to 12v, to find out the value of surface roughness and material removal at each electrochemical state. From the measured material removal for each process state was used to verify the relationship with finishing time of work piece. Electrochemical finishing proves an effective method to reduce the surface roughness ( $R_a$ ) from  $1.6\mu\text{m}$  to  $0.1\mu\text{m}$  in 4 min. Finally, the observed relationships were used to predicate the diameter of blank, tool diameter and flow rate by neural network modeling ANN which has inputs defined by the finished hole diameter, surface roughness, and finishing time. Three of hidden layers and their neurons were found by an integration procedure. The design charts observed from this study utilize the designers in predication of diameter for blank and design of electrode.

**Keywords:** Design; Electrode; Electrochemical; Polishing; Roughness

### Introduction

Polishing is a tedious and necessary finishing operation for many products. The manual operations of grinding and polishing labor intensive and prompt for human error. The other mechanical polishing methods such as shot peening and sand blasting were rough and imprecise. The chemical etching-polishing methods were simple and cost effective. However, they are environmental safe. The finished surface may not meet surface quality requirements, Shuo-Jen Lee 2003. [1]

The applications of electrochemical machining technology have been established in specific industries and

products. The ECM technology had been used in the production of spur gears of the automobile and the turbine blades of an aircraft.

Pa, 2010 studied a novel finishing tool was developed by using the two finishing processes of burnishing and electrochemical finishing. The finishing tool design included a burnishing tool and an electrode as a bore surface finish improvement, which goes beyond traditional boring by utilizing the continuous processes of burnishing and electrochemical finishing. Only a short time is required to make the bore surface smooth and bright with the use of these continuous

finishing processes. The experimental results show that the large current rating is closely concerned with the fast feed rate of the finishing tool and is advantageous to the finishing processes. A small end radius or a small thickness of the electrode provides a more sufficient discharge, which is advantageous for the finish. The finishing effect is better with a high rotational speed of the finishing tool, since the dress discharge the electrochemical machining, and burnishing becomes easier, which is also advantageous to the finishing processes. The finishing time using continuous current was not as prolonged as with the pulsed current.

Ning Ma et al, 2010 [3] studied the anodic smoothing characteristics of PECF. They analyzed through a developed mathematical model. In their study, the main influencing factors such as the finishing time, the inter electrode gap, the applied voltage and the rotational speed of electrode have been examined. The predictive values based on the developed mathematical model are found to be in reasonable agreement with the experimental values. The surface roughness  $R_z$  ranges from  $3\mu\text{m}$  to  $1.22\mu\text{m}$ . The research achievement through various parametric studies can be used as a guideline for the operation of a PECF system.

Maksoud and Brooks, 1995 [4] reported grinding of ceramic form tooling with diamond powder and electrochemical technology. De Silva and McGeough 1989, conducted pulsed power supply of ECM technology for micromachining.

Choi and Kim, 1998 [6] employed electroplated CBN wheel for electrochemical deburring. The operating voltage and current density of above ECM applications were generally high. The metal removal rate (machining) is important. It operates at

the metallic dissolution of the electrochemical reaction. Those process parameters were too high for polishing purpose. Operating at lower range of voltage and current density, the electrochemical reaction exhibits passive characteristics.

The electrochemical polishing mechanisms of the electrochemical mechanical polishing were studied with linear polarization method and Faraday's law on the SKD11 tooling steel. The linear polarization method has been widely employed to characterize the electrochemical properties of a material after surface treatment.

Cai et al, 2003 [7] used I-V curves to characterize the changes in electrochemical and anti-corrosion properties after sand blasting and mechanical polishing of the titanium alloys.

### Experimental Work

Fig. 1 shows the set-up of the electrochemical finishing system (ECF) for carrying out finishing operations on the inner surface of tube with diameter  $D$ .

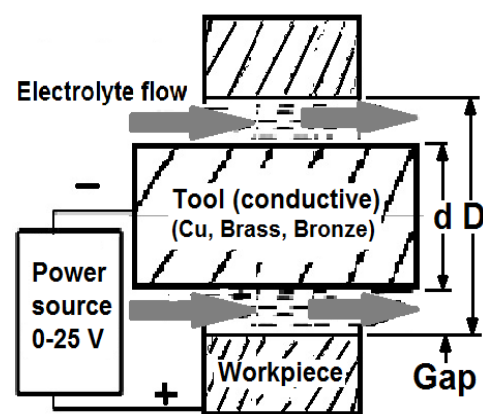


Fig. 1, The set-up of the electrochemical system

The work piece and the tool are being securely held by a three-jaw chuck and a clamp respectively, on convention machine type (SIG) as shown in Fig. 2. Both the work piece and the tool are insulated from the main body in order to only focus an

electrochemical reaction between the work piece and the tool. For using a fixed electrode in ECF, the working area of electrode is larger than the machined area, in the work piece.



Fig. 2 The set-up of the work piece

Composition of work piece is given in Table (1). The raw material comes in the form of extruded bar with a diameter of 30 and 50mm. Before drilling, the bar was faced by turning.

Table 1, Composition of work piece

C (%)	Si (%)	Mn(%)	Cr (%)
0.86	0.40	0.45	0.05
Mo (%)	Co (%)	Fe	
4.5	4.0	Balance	

As given in Table (2) the samples for this study, were drilled with  $D_{blank}$  as shown in Fig. 3 in order to evaluate the influence of electrochemical finishing on surface, as material removal in  $mm^3$  and surface roughness  $R_a$  in  $\mu m$ .

Experiments have been carried out on a developed ECF-setup to evaluate the influences of some process parameters on surface roughness and dimensions of holes.

In this study, three predominant machining parameters are involved. They are flow rate of electrolyte, machining voltage and finishing time.

Table 2, Groups of specimens

Dia. Of blank (mm)	Electrolyte Flow rate (lit/min)	Voltage (volt)			
		6	8	10	12
5	5	6	8	10	12
	10	6	8	10	12
	15	6	8	10	12
10	5	6	8	10	12
	10	6	8	10	12
	15	6	8	10	12
15	5	6	8	10	12
	10	6	8	10	12
	15	6	8	10	12

Cells with gray color were predated by ANN

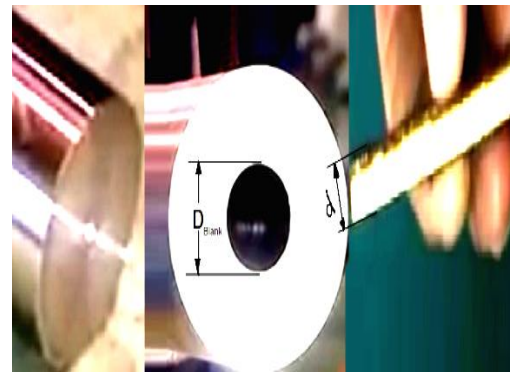


Fig. 3, The set-up of the blank and electrode

## Results and Discussion

### 1. Surface roughness.

Fig. 4 to Fig. 12 shows the influences of the finishing time on the surface roughness ( $R_a$ ) of holes, for different voltage. It can be observed from Fig.4 that the surface roughness ( $R_a$ ) decreases with the finishing time and with applied voltage value at a particular parametric combination, i.e. diameter of blank, 5mm; flow rate of electrolyte, 5 l/min. Due to the increase in applied voltage, the machining current also increases. According to Faraday's law, the material removal rate is proportional to the machining current. However, Fig.4 obviously indicates that the surface roughness ( $R_a$ ) of machined hole was varied linearly. As shown in Fig.4, the  $R_a$  of hole from 6V decreases less rapidly than in the voltage of 8V. From 10V, the  $R_a$  decreases more rapidly than in the

voltage of 8V. From 12V, the  $R_a$  decreases more rapidly than in the voltage of 10V. With the increase of applied voltage, current density increases. These trends are the consequences of less increment of dissolution efficiency at low voltage range, i.e. between 6 to 12V.

By comparison, in the range of 6 to 12V, the efficiency increment rate is more and the dissolution efficiency reaches towards its maximum value. Consequently, the  $R_a$  of finished-hole decreases with applied voltage. For example, when the applied voltage is 6V, the  $R_a$  can change from 1.6 to 0.1  $\mu\text{m}$ . When the applied voltage is 12V, the  $R_a$  can change from 1.6 to 0.05  $\mu\text{m}$ , with flow rate 5 l/min and finishing time 4 minutes for both cases. As shown in Figs. from 4 to 12.

As given in table (2) the samples for this study, were drilled with  $D_{\text{blank}}$  in order to evaluate the influence of electrochemical finishing on surface, as material removal in  $\text{mm}^3$  and surface roughness  $R_a$  in  $\mu\text{m}$ . From a tool design standpoint, it is also of interest to be able to predict recommended operating conditions and the optimal tool diameter  $d$ , with future quantities based on experimental data and requirement of finishing  $R_a$ , due prediction by neural network modeling ANN.

Finishing of surface ( $R_a$ ) is commonly described by parameters such as the centre-line-average or roughness average (CLA or 'Ra'),  $R_a$  is the universally recognized parameter of roughness. It is the arithmetical mean of the departures of the profile from the mean line, so that:

$$R_a = \frac{1}{L} \int_0^L |z| dx \quad \dots(1)$$

Where: L is the sampling length (m); z is the height of the profile along 'x' (m) as shown in Fig. 13.

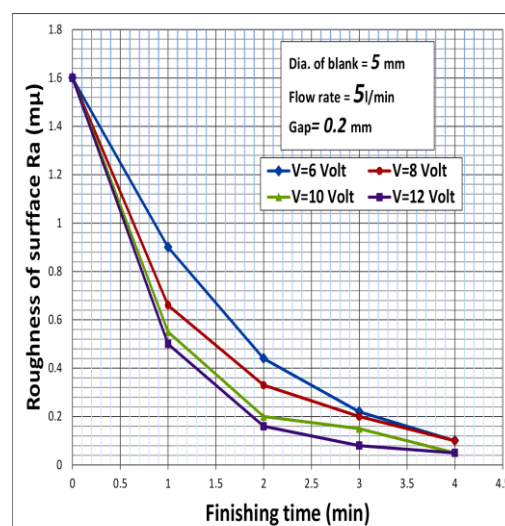


Fig. 4, The relation between finishing time and  $R_a$  for  $D_{\text{Blank}}$  5mm with 5 liter/min flow rate

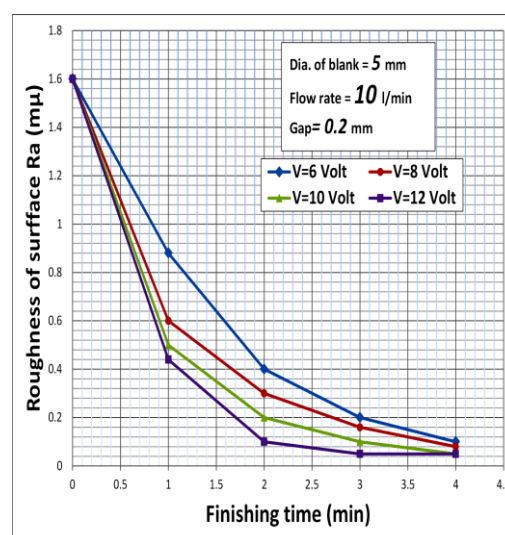


Fig. 5, The relation between finishing time and  $R_a$  for  $D_{\text{Blank}}$  5mm with 10 liter/min flow rate

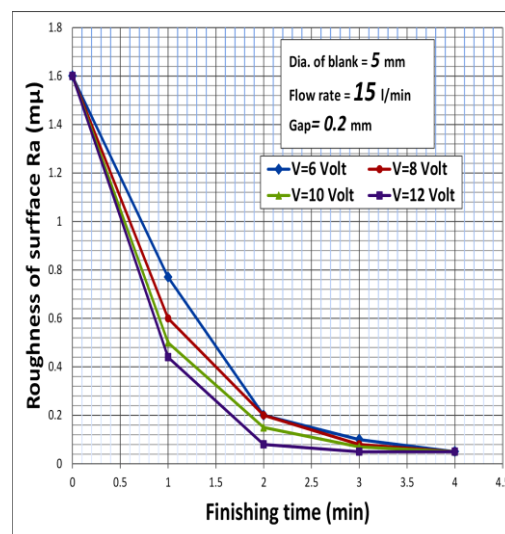


Fig. 6, The relation between finishing time and  $R_a$  for  $D_{\text{Blank}}$  5mm with 15 liter/min flow rate

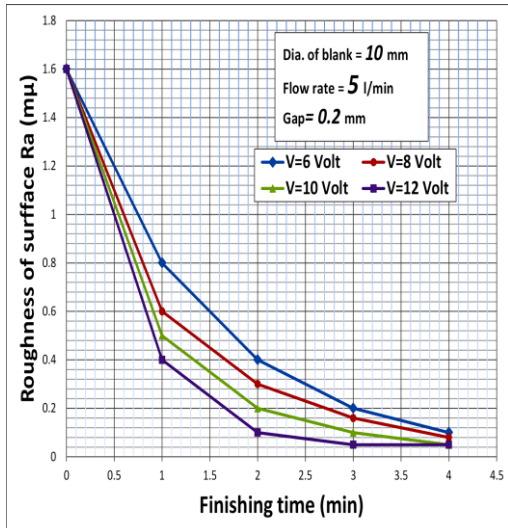


Fig. 7, The relation between finishing time and Ra for  $D_{Blank}$  10mm with 5 liter/min flow rate

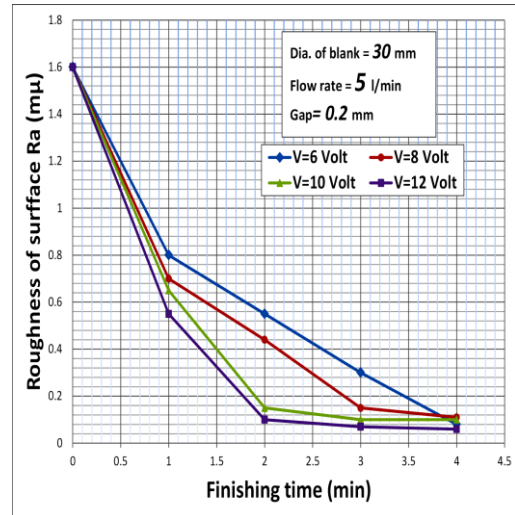


Fig. 10, The relation between finishing time and Ra for  $D_{Blank}$  30mm with 5 liter/min flow rate

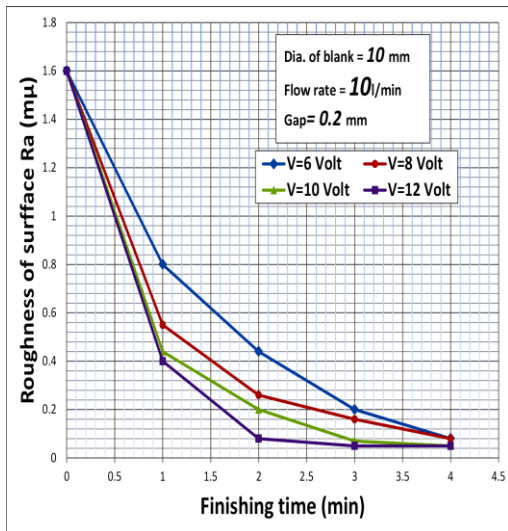


Fig. 8, The relation between finishing time and Ra for  $D_{Blank}$  10mm with 10 l/min flow rate

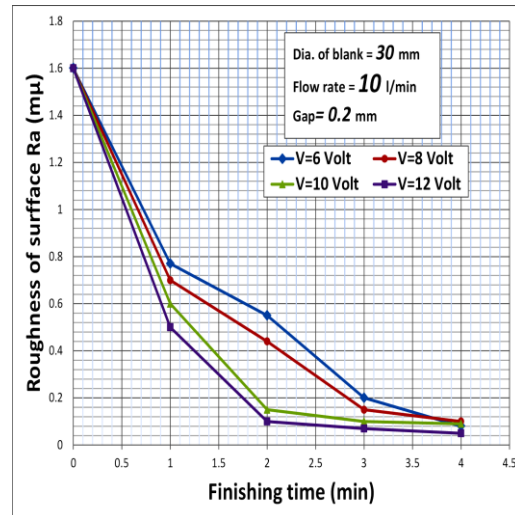


Fig. 11, The relation between finishing time and Ra for  $D_{Blank}$  30mm with 10 l/min flow rate

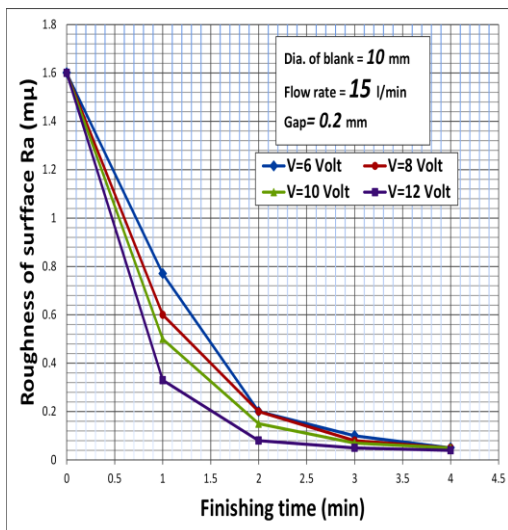


Fig. 9, The relation between finishing time and Ra for  $D_{Blank}$  10mm with 15 liter/min

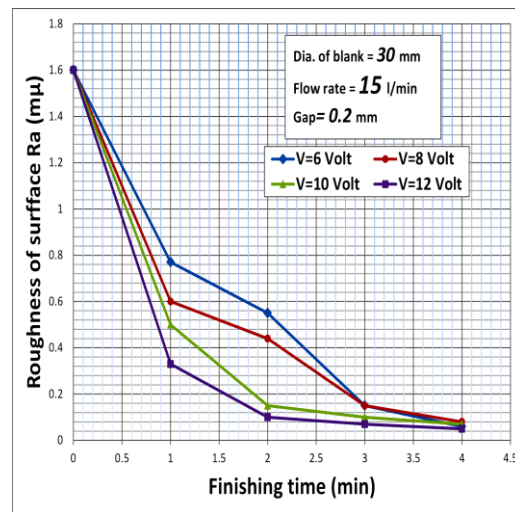


Fig. 12, The relation between finishing time and Ra for  $D_{Blank}$  30mm with 15 l/min flow rate

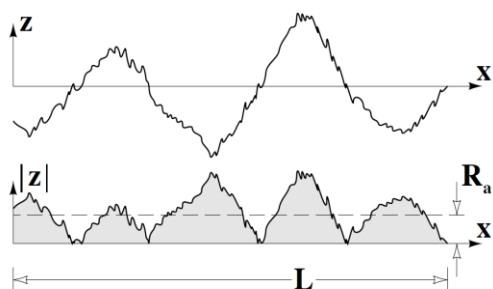


Fig. 13, The roughness average

The blank was drilled with hole larger than the diameter of electrode (d) as shown in Fig. 3, thus:

$$D_{\text{blank}} = d + 2 \text{ Gap} \quad \dots (2)$$

$$\text{Finished Dia. (D)} = D_{\text{blank}} + T \quad \dots (3)$$

Where: Gap is the distance between surface of tool (electrode) and the inner surface blank, d is the diameter of electrode. T is the thickness of removal layer from inner surface, as:

$$T = MR_{\text{total}} / \pi DL \quad \dots (4)$$

Where: L is the length of work piece.

The anode material dissolved electrochemically is flushed away by flowing electrolyte (typically NaCl and NaNO<sub>3</sub> aqueous solution). With the continuous feeding of the tool, the shape produced in the work piece is nearly a negative mirror of the tool electrode, Zhiyong Li [9].

## 2. Material removal

Figs. from 14 to 22 show the effect of finishing time on the material removal value, for different of applied voltage at a particular machining condition, i.e. applied voltage machining voltage of 6V and flow rate of electrolyte, 5 l/min. The nature of curve is almost linear at one period, i.e. from 1 min to 2 min. The increment of material removal at high voltage case, i.e. from 6v to 12v, is more and so the material removal varies from 80 mm<sup>3</sup> to 110 mm<sup>3</sup>, for 5mm diameter, at 5 l/min flow rate of electrolyte.

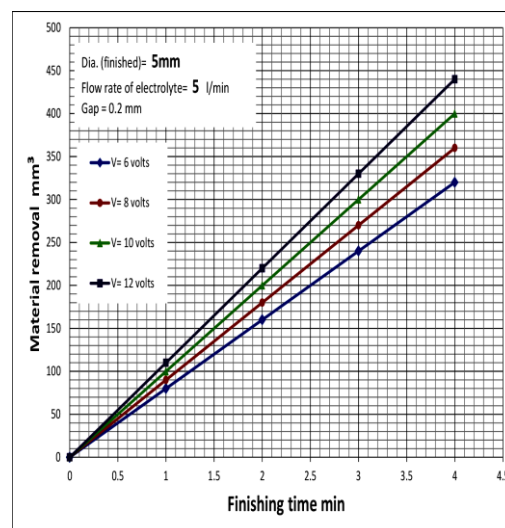


Fig. 14, The material removal with finishing time for D<sub>Blank</sub> 5mm and Q=5 l/min

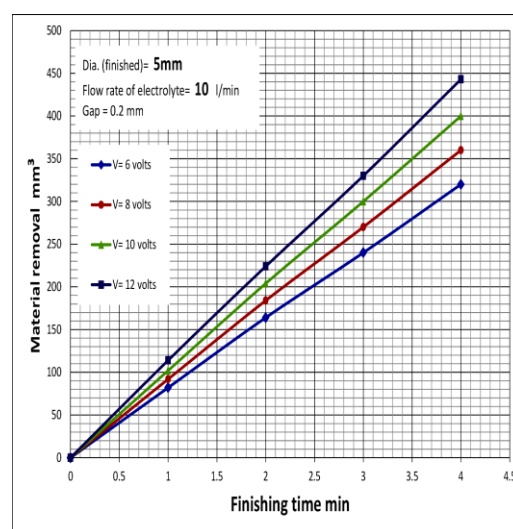


Fig. 15, The material removal with finishing time for D<sub>Blank</sub> 5mm and Q=10 l/min

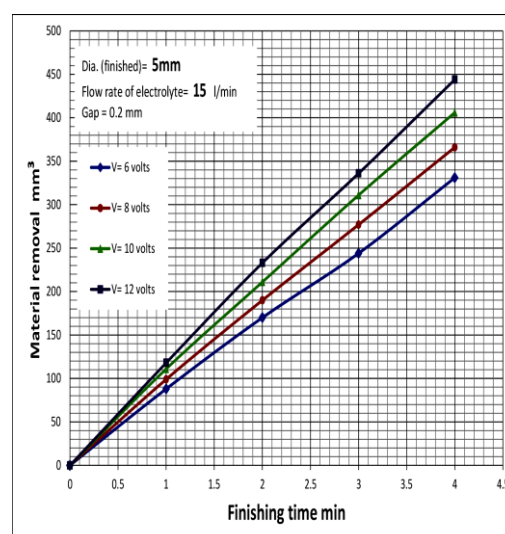
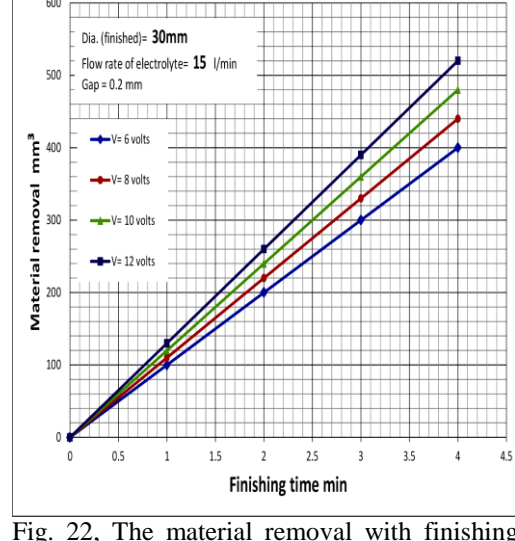
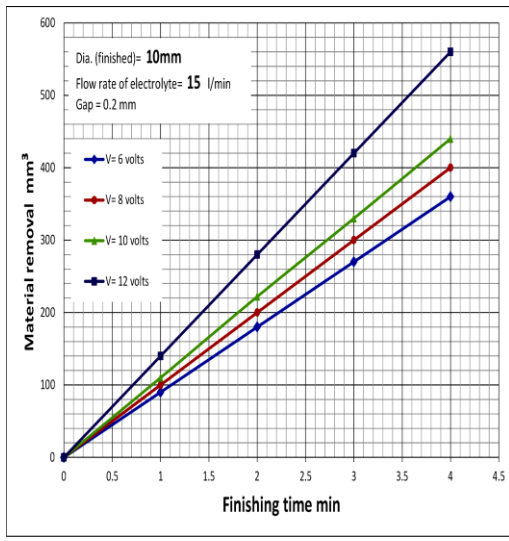
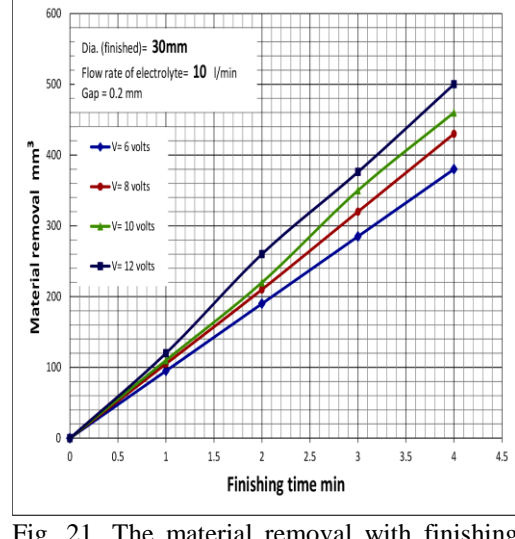
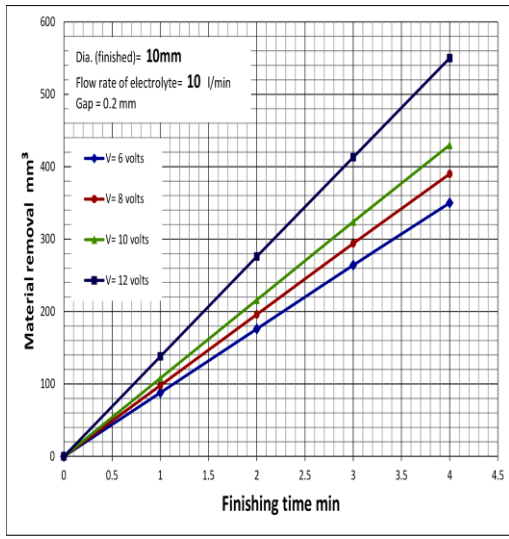
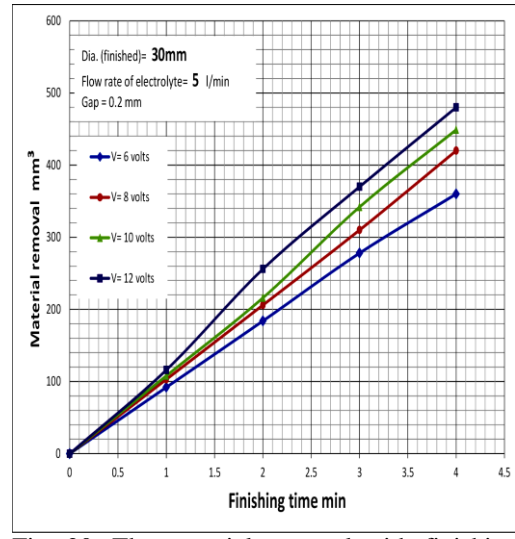
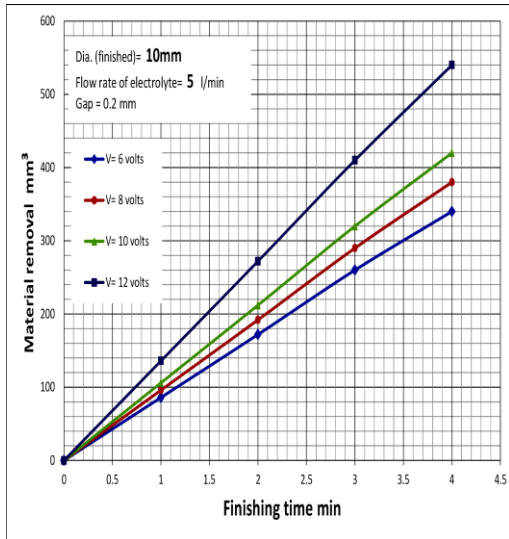


Fig. 16, The material removal with finishing time for D<sub>Blank</sub> 5mm and Q=15 l/min



In high applied voltage, the large number of ions associated in the machining process increases the machining current density and thus results in the larger diameter of hole. Furthermore, the experimental results also demonstrate that material removal. The diameter of machined holes with different flow rate of electrolyte is shown in Figs. from 14 to 22. It is clear from figures that the increasing for value of removal material, with the increase of the applied flow rate of electrolyte increase.

Material removal rate (MRR) is an important characteristic to evaluate efficiency of a non-traditional machining process. In ECM, material removal takes place due to atomic dissolution of work material. Electrochemical dissolution is governed by Faraday's laws. The first law states that the amount of electrochemical dissolution or deposition is proportional to amount of charge passed through the electrochemical cell, which may be expressed as:

$$M \propto Q \quad \dots(5)$$

Where:  $m$  = mass of material dissolved or deposited,  $Q$  = amount of charge passed.

The second law states that the amount of material deposited or dissolved further depends on Electrochemical Equivalence (ECE) of the material that is again the ratio atomic weight and valiancy. Thus

$$m \propto ECE \propto A/v \quad \dots(6)$$

Where: ECE= Electrochemical Equivalence,  $A$ =the atomic weights,  $v$ = valiancy, Thus:

$$m \propto (QA)/v \quad \dots(7)$$

$$m = ItA/(Fv) \quad \dots(8)$$

Where:  $F$ = Faraday's constant =96500 coulombs,  $I$ = current,  $t$ = time.

$$MRR = m/(pt) = IA/(Fpv) \quad \dots(9)$$

Where MRR = Material removal rate,  $\rho$ = density of the material.

The engineering materials are quite often alloys rather than element consisting of different elements in a given proportion.

Let us assume there are 'n' elements in an alloy. The atomic weights are given as  $A_1, A_2, A_n$  with valiancy during electrochemical dissolution as  $v_1, v_2, \dots, v_n$ . The weight percentages of different elements are  $\alpha_1, \alpha_2, \alpha_n$  (in decimal fraction)

Now for passing a current of  $I$  for a time  $t$ , the mass of material dissolved for any element 'i' is given by:

$$m_i = \Gamma_a \rho \alpha_i \quad \dots(10)$$

Where  $\Gamma_a$  is the total volume of alloy dissolved. Each element present in the alloy takes a certain amount of charge to dissolve

$$m_i = Q_i A_i / (F v_i) \quad \dots(11)$$

$$Q_i = F m_i v_i / A_i \quad \dots(12)$$

$$Q_i = F \Gamma_a \rho \alpha_i v_i / A_i \quad \dots(13)$$

The total charge passed=  $\sum Q_i$

$$Q_T = I t \quad \dots(14)$$

$$Q_T = F \Gamma_a \rho \sum \alpha_i v_i / A_i \quad \dots(15)$$

Now:

$$MRR = \Gamma_a / t \quad \dots(16)$$

$$MRR = \frac{\Gamma_a}{t} = \frac{1}{F\rho} \cdot \frac{I}{\sum \frac{\alpha_i v_i}{A_i}} \quad \dots(17)$$



The material removal from surface produced a new surface with smoothness, as shown in Fig. 23.

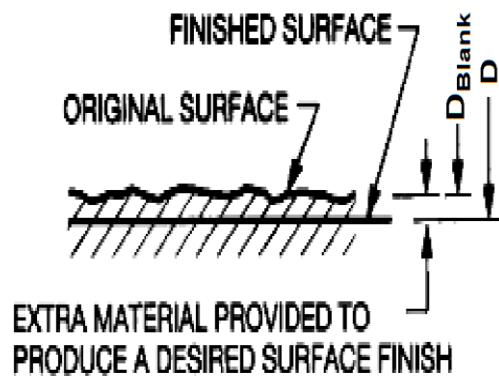


Fig. 23, The relation between finished and original surfaces

Air bubbles also sometimes accompany the electrolyte due to the improper control of electrolyte flow and other gas bubbles like H<sub>2</sub> are generated during the electrochemical process. Zhiyong Li [10].

Fig. 24 shows a sample of the relationship between the gap value and material removal. The gap affect on material removal was studied with same manner, for gap 0.2, 0.4, 0.6 and 1.0mm. A sample of these results.

Due to Fig. 23, which is show the surface topography of workpiece before and after ECF. It can be found that the surface topography finished by ECF is much different from original mechanically machined surface profile. As shown in Fig. 23, wave crests of original mechanically machined surface profile disappear quickly after ECF. This is mainly due to the concentration of current lines on wave crests of a surface profile thus leading to a locally higher dissolution rate Landlot [11] and other researcher [12-18], which is popularly considered.

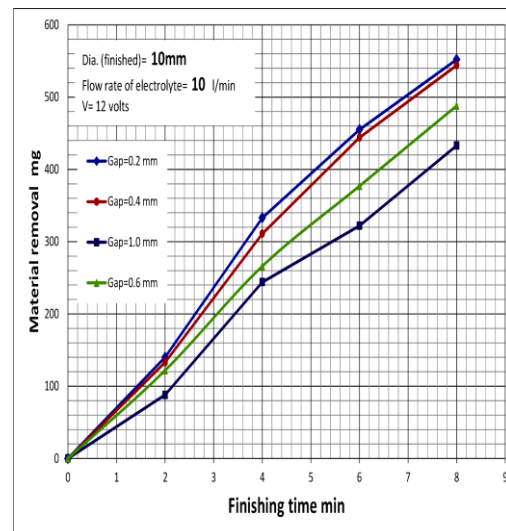


Fig. 24, A sample of the relation between finishing time and material removal for Dia.10mm

### 3. Optimal design by ANN.

The previous results in this study were used in order to evaluate the technical requirement; recommended operating conditions, diameter of the blank  $D_{\text{blank}}$ , diameter of the electrode. The recommended operating conditions; applied voltage, electrolyte flow rate (liter/min) and the gap.

The influence of electrochemical finishing on surface; material removal in  $\text{mm}^3$  and surface roughness  $R_a$  in  $\mu\text{m}$ . These experimental data were used as input data, for ANN programming, with operating conditions for each state.

From a tool design standpoint, it is also of interest to be able to predict the recommended operating conditions, for the required finished surface roughness. The first stage of the ANN resultants is the fixing of the recommended operating conditions for required finished surface roughness. Secondly, the thickness of material removal was estimate, to predicate the tool diameter  $d$ , due to the technical recommendation and design requirements, based on experimental data, with predication by neural network modelling ANN.

The input-output mapping of a multi-layer perceptron is established according to requirements of this study, Fig. 25 show the block-diagram for modeling and program, consist of inputs which are defined by finished hole diameter (D), surface roughness (Ra), and finishing time (t). Network outputs were defined by diameter of blank ( $D_{Blank}$ ), tool diameter (d), and flow rate (Q). Data sets was clustered and grouped as a combination based on other variables (e.g. gap, applied voltage,...etc).

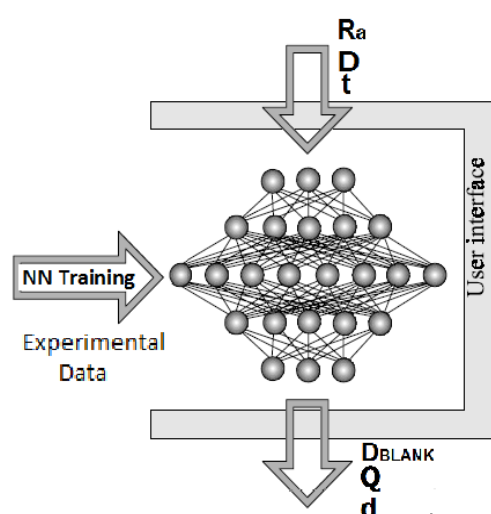


Fig. 25, Multi-layers; input, output and hidden

Initially, the number of neurons in hidden layer was found by an iteration procedure, in which 3 hidden layers was assumed, each consist of 50 neurons. Training procedure was performed and the resulting performance index was saved. Then, the number of neurons was reduced by one. Training procedure was performed again and the resulting performance index was compared with the previous one. This procedure was repeated until minimum performance index was found. In this study, neural networks have three hidden layers with the number of neurons being approximately between 5 and 27 and at most two hidden layers with 8 fixed neurons in the second layer and the

number of neurons in the third layer being between 5 and 10. MATLAB neural network toolbox was used to create and train networks as shown in appendix A. Fig. 26 show the ordinary operations of classic design before ANN. The observed data from experiment work was used for training of ANN. Table (3) show the structures and performances of Neural Networks.

Table 3, Performances of Neural Networks

Training algorithm	No. training epochs	Mean squared error MSE	R correlation coefficient
Gradient descent method	88	2.961314 e-002	0.99854

Figs. 27 to 33 show samples of the ANN resultants, as design charts. The operating conditions and required finished surface roughness should be estimated, firstly, in tool design process. Secondly, use these design charts, to estimate the tool diameter d and diameter of blank, due to these charts.

The new data, in this study, was predicated by using neural network method. The predication based on previous works of other many researchers; Hu'sken et al 2005 [20], studied the structure optimization of neural networks for evolutionary design optimization. They studied the use of neural networks as approximate models for the fitness evaluation in evolutionary design optimization.

Xiaoyu, 2008 [21], estimated the tool wear modeling in hard turning by using neural network. The estimation was based on a fully forward connected neural network with cutting conditions and machining time as the inputs and tool flank wear as the output.

Paulo R. Aguiar et al 2008 [22], they used the grinding parameters as input to the neural network, which have not been tested yet in surface roughness

prediction by neural networks. Besides, a high sampling rate data acquisition system was employed to acquire the acoustic emission and cutting power.

Qing-hua Yang et al 2012 [23], studied the optimum design of combined cold extrusion die for bevel gear by using neural network. Neural network is used to establish mapping relationship between die and process parameters and maximum extrusion force.

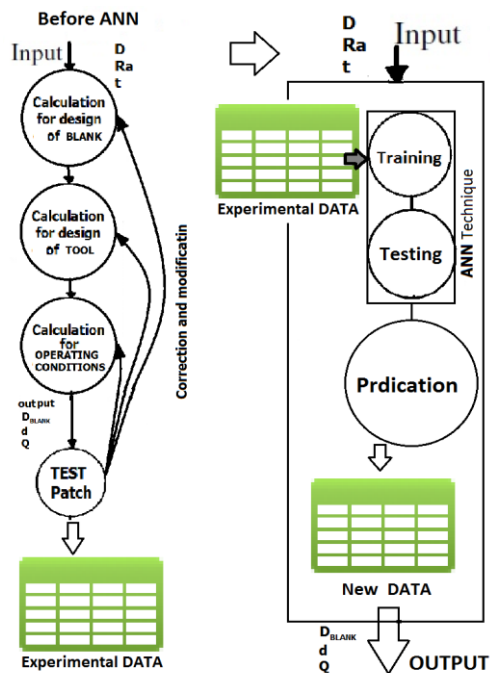


Fig. 26, The design operations before and after ANN

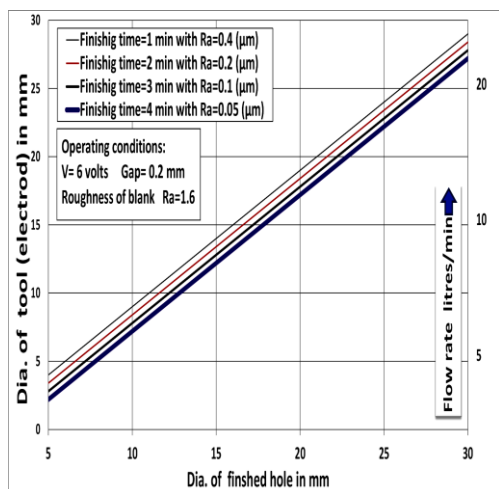


Fig. 27, Design chart of electrode at applied voltage 6v and gap 0.2mm

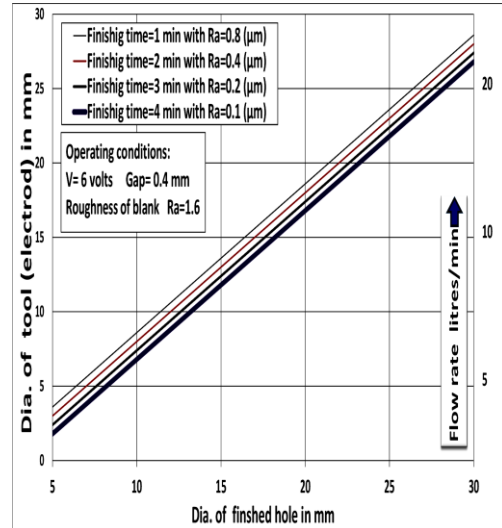


Fig. 28, Design chart of electrode at applied voltage 6v and gap 0.4mm

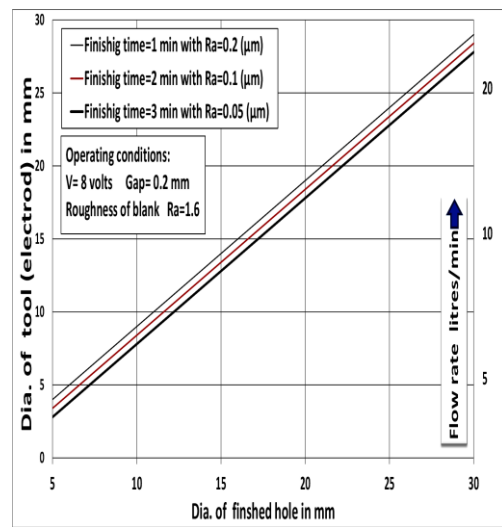


Fig. 29, Design chart of electrode at applied voltage 8v and gap 0.2mm

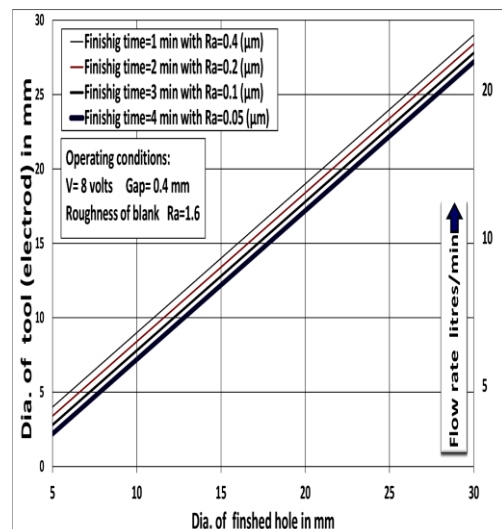


Fig. 30, Design chart of electrode at applied voltage 8v and gap 0.4mm

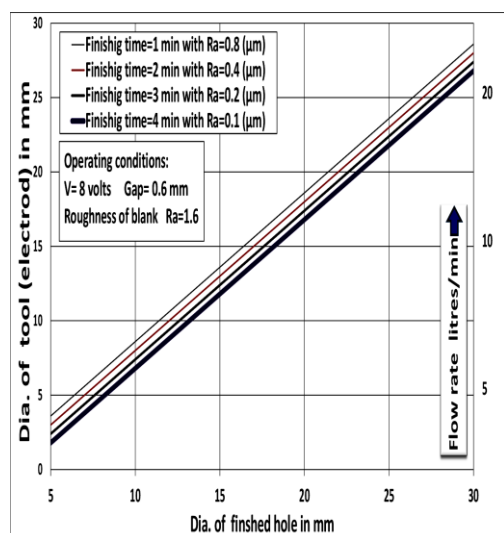


Fig. 31, Design chart of electrode at applied voltage 8v and gap 0.6mm

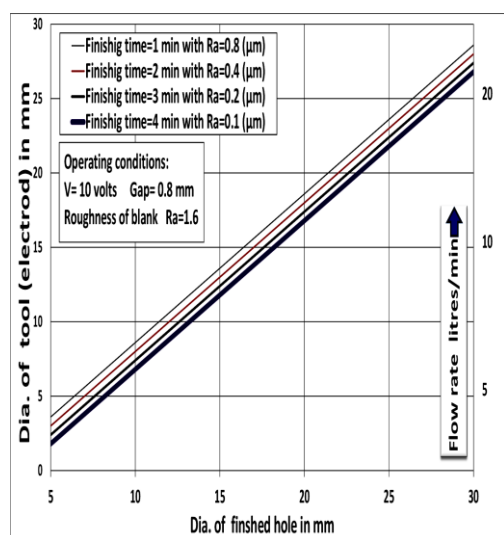


Fig. 32, Design chart of electrode at applied voltage 10v and gap 0.8mm

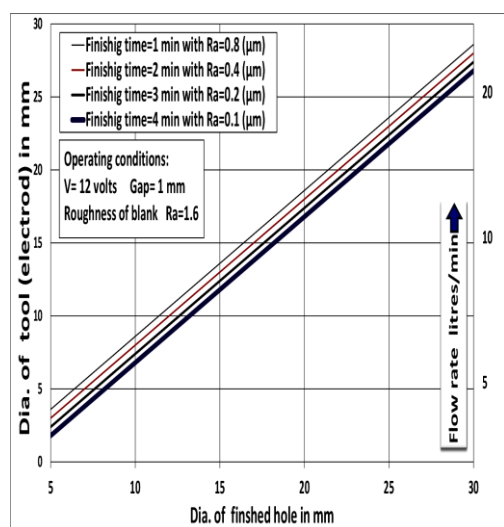


Fig. 33, Design chart of electrode at applied voltage 12v and gap 1.0mm

Fig. 34 shows final design chart, due to optimization of Figs. From 27 to 33, by ANN modeling based on the technical recommendation (applied voltage, value of gap and flow rate of electrolyte) and design requirements (finished diameter  $D$  and  $R_a$  of finished surface), based on experimental data, with extended range, using predication by neural network modeling ANN.

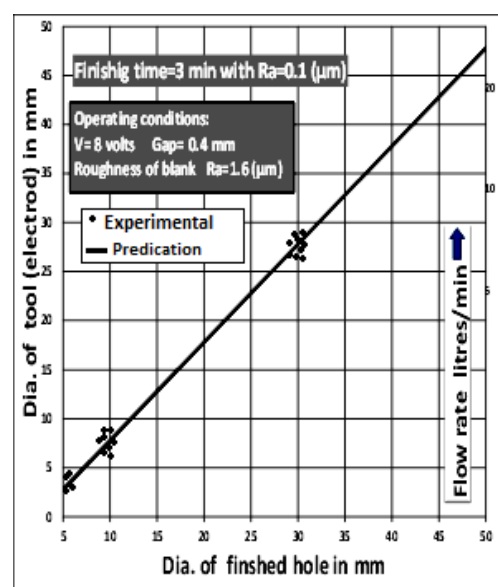


Fig. 34, Design chart of electrode at recommended conditions

In comparing the results of this study with those of reference [1, 17], the operating condition and finishing requirement were considered respectively. And in comparing the numerical results of ANN modeling of predication for  $D_{Blank}$  and Dia of tool ( $d$ ), that are obtained from ANN technique.

### Conclusions

In the present work, an idealized design of electrode, for mass production has been developed and verified experiments have been performed with different finishing parameters. Some key findings the experimental investigation are listed as follows:

- 1) Electrochemical finishing (ECF) proves an effective method to reduce the surface roughness  $R_a$  from  $1.6\mu\text{m}$  to  $0.1\mu\text{m}$  in 4 min.
- 2) In order to reduce several microns of the maximum height of the profile, it needs to remove a few hundred of microns from the workpiece surface. For example, the total removal thickness is equal to  $300\mu\text{m}$  in order to reduce the  $R_a$  from  $1.6\mu\text{m}$  to  $0.1\mu\text{m}$  in 4 min.
- 3) For good surface quality, it was suggested to operate at applied voltage 12v and flow rate of electrolyte of 15 liter.
- 4) It is easily implemented as a generalized system of design for tool, based on neural network, system has an open structure which enables improvements and further revisions of knowledge bases.
- 5) A collaborative optimization method for the design of electrochemical polishing requirement is presented in this paper, combined using design knowledge (know-how), experimental data and the predication and optimization capability of neural network.

### Nomenclature

ECF: Electrochemical finishing.

ECM: Electrochemical machining.

PECF: Pulse electrochemical finishing.

ANN: Artificial neural network.

MRR: Material removal rate ( $\text{mm}^3/\text{min}$ ).

MRR: Material removal ( $\text{mm}^3$ ).

$D_{\text{Blank}}$ : Diameter of blank.

$d$  : Diameter of tool.

$D$  : Diameter of finished hole.

$R_a$  : Surface roughness.

SKD11: Tooling steel with high chrome.

$R$  : Correlation coefficient.

MSE : Mean squared error.

### References

- 1- Shuo-Jen Lee, Yu-Ming Lee, Ming-Feng Du, "The polishing mechanism of electrochemical mechanical polishing technology", *Journal of Materials Processing Technology* 140 (2003) 280–286.
- 2- P. S. Pa, "Continuous finishing processes using a combination of burnishing and electrochemical finishing on bore surfaces", *Int J Adv Manuf Technol* (2010) 49:147–154.
- 3- Ning Ma, Wenji Xu, Xuyue Wang, Bin Tao, "Pulse electrochemical finishing: Modeling and experiment" *Journal of Materials Processing Technology* 210 (2010) 852–857.
- 4- T.M.A. Maksud, A.J. Brooks, "Electrochemical grinding of ceramic form tooling", *Journal of Materials Processing Technology*. (1995) 70–75.
- 5- A.K.M. De Silva, J.A. McGeough, "Process monitoring of electrochemical micromachining", *J. Mater. Process. Technol.* (1998) 165–169.
- 6- I.-H. Choi, J.-D. Kim, "Electrochemical deburring system using electroplated CBN wheels", *Int. J. Mach. Tools Manuf.* 38 (1–2) (1998) 29–40.
- 7- Z. Cai, T. Shafer, et al., "Electrochemical characterization of cast titanium alloys", *Biomaterials* (2003) 213–218.
- 8- D.A. Jones, A.J.P. Paul, "Acid leaching behavior of sulfide and oxide minerals determined by electrochemical polarization measurements", *Miner. Eng.* 8 (4–5) (1995) 511–521.
- 9- Zhiyong Li, Di Zhu, Numerical solution for cathode design of aero-engine blades in electrochemical machining, *The IEEE international conference on mechatronics and*

- automation, 2006, Volume 2:1418~1423.
- 10- Zhiyong Li, Guangming Yuan, "Experimental Investigation of Micro -holes in Electrochemical Machining Using Pulse Current" Proceedings of the 3rd IEEE Int. Conf. on Nano/Micro Engineered and Molecular Systems, January 6-9, 2008, (IVSL).
- 11- Landolt, D., Chauvy, P.F., Zinger, O., 2003. "Electrochemical micromachining, polishing and surface structuring of metals: fundamental aspects and new developments." *Electrochem. Acta* 48, 3185–3201.
- 12- Mahdavinejad, R., Hatami, M., 2008. "On the application of electrochemical machining for inner surface polishing of gun barrel chamber", *J. Mater. Process. Technol.* 202, 307–315.
- 13- Masuzawa, T., Sakai, S., 1987. "Quick finishing of WEDM products by ECM using a mate-electrode", *Ann. CIRP* 36 (1), 123–126.
- 14- McGeough, J.A., "Principles of Electrochemical Machining. Chapman and Hall, London. ", 1974.
- 15- Pa, P.S., 2008. "Effective form design of electrode in electrochemical smoothing of end turning surface finishing." *J. Mater. Process. Technol.* 195, 44–52.
- 16- Phillips, R.E., "What is electrochemical grinding and how does it work. Carbide", 1986. *Tool J.* 18 (6), 12–14.
- 17- Rajurkar, K.P., Kozak, J., Wei, B., McGeough, J.A., 1993. "Study of pulse electrochemical machining characteristics.", *Ann. CIRP* 42 (1), 231–234.
- 18- Rajurkar, K.P., Wei, B., Kozak, J., McGeough, J.A., 1995. "Modelling and monitoring interelectrode gap in pulse electrochemical machining." *Ann. CIRP* 44 (1), 177–180.
- 19- Ning Ma, Wenji Xu, Xuyue Wang, Bin Tao, "Pulse electrochemical finishing: Modeling and experiment" *Journal of Materials Processing Technology* 210 (2010) 852–857.
- 20- Hu'sken, M.Y. Jin, B. Sendhoff, 'structure optimization of neural networks for evolutionary design optimization', *Soft Computing* 9 (2005) 21–28.
- 21- Xiaoyu Wang, Wen Wang, Yong Huang, Nhan Nguyen, Kalmanje Krishnakumar, "Design of neural network-based estimator for tool wear modeling in hard turning", *J Intell Manuf* (2008).
- 22- Paulo R. Aguiar, Carlos E. D. Cruz, Wallace C. F. Paula and Eduardo C. Bianchi 'Predicting Surface Roughness in Grinding Using Neural Networks', *Advances in Robotics Automation and Control*, ISBN: 978-953-7619-16-9,(2008).  
<http://www.intechopen.com>
- 23- Qing-hua Yang, Xin Chen, Bin Meng, and Juan Pan, 'optimum design of combined cold extrusion die for bevel gear', *International Journal of Engineering and Technology*, Vol. 4, No. 4, August 2012.

#### Appendix A:

##### Neural Networks Program

```
DataFileName='nad1';
OP_File_Name=[DataFileName
'_Results'];
Data=xlsread(DataFileName);
[ROW,COLOM]=size(data);
Ra=data(2:ROW,1);
t= data (1,2:COLOM);
D= data (2:ROW,2:COLOM)';
Q=data(2:ROW,1);
Db= data (1,2:COLOM);
d= data (2:ROW,2:COLOM);
IP=[];Target=[];
```

```
IP=[Ra;t;D];
Target=[Q,Dp,d];
PR=[min(Ra) max(Ra);min(t) max(t)
);min(D) max(D)];
LayerSize=[No_Of_Neurons];
net = newff(PR,LayerSize,{'tansig'
'purelin'});
net = train(net,IP,Target);
Y = sim(net,IP);
ddd=xlswrite(nadhun1.xls,Y)
```